Int. J. Heat Mass Transfer. Vol. 31, No. 12, pp. 2590–2593, 1988
Printed in Great Britain

0017–9310/88 $3.00 + 0.00

Developing laminar flow and heat transfer in the entrance region of regular polygonal ducts

YUTAKA ASAKO and HIROSHI NAKAMURA
Department of Mechanical Engineering, Tokyo Metropolitan University, Tokyo, Japan

and

MOHAMMAD FAGHRI
Department of Mechanical Engineering and Applied Mechanics, University of Rhode Island, Kingston, RI 02881, U.S.A.

(*Received* 9 *June* 1987 *and in final form* 6 *May* 1988)

INTRODUCTION

A SUMMARY of the literature on heat transfer in laminar duct flows has been brought together in a book by Shah and London [1]. From a study of this information, it is apparent that only limited consideration has been given to three-dimensional duct problems. The pioneering work is by Patankar and Spalding [2] who developed a calculation procedure for three-dimensional parabolic flows. This procedure was adopted by Prakash and Liu [3] and Karki and Patankar [4] to duct problems with a regular cross-section. Recently, Lawal and Mujumdar [5] have developed a calculation procedure for three-dimensional parabolic flows in ducts with irregular cross-section. They coupled the calculation procedure for three-dimensional parabolic flows with the orthogonal coordinate transformation methodology to obtain results for the entrance region of a regular pentagonal duct. A careful search of the literature failed to disclose any other prior work on the hydrodynamic and thermal entrance characteristics of ducts with irregular cross-section. This is with the exception of the recent study [6] which has developed a solution methodology to obtain three-dimensional fluid flow and heat transfer characteristics in the entrance region of a rhombic duct. The methodology is applied to a regular polygonal duct in this work.

The numerical methodology that was used in this paper utilizes an algebraic coordinate transformation developed in previous papers [7, 8] which maps an irregular cross-section onto a rectangle. This method was coupled with the calculation procedure for three-dimensional parabolic problems by ref. [2]. The numerical solutions were carried out for both uniform wall temperature and uniform wall heat flux and for hexagonal, octagonal, square, and circular ducts. The solutions were obtained for developing flow and for two Prandtl numbers ($Pr = 0.7$ and 8). The thermal entrance solutions were also obtained for slug flow and for fully developed flow.

FORMULATION

Description of the problem

The problem to be considered in this study is schematically depicted in Fig. 1(a). It involves the determination of three-dimensional heat transfer and fluid flow characteristics for laminar, incompressible, forced convection in the entrance region of a general n-sided polygonal duct. As seen in this figure, the fluid enters with a uniform velocity $\bar{w}$ and a uniform temperature T_i. Two types of thermal boundary conditions are considered. These are a uniform heat input per unit axial length with a uniform temperature at any cross-section and a uniform temperature both axially and peripherally. These are the *H1* and *T* boundary conditions, respectively, of Shah and London [1]. Figure 1(b) pictures the cross-section of the duct. As seen there, the top and bottom walls lie along the x-axis while the other walls do not lie along the y-axis. The half width of the cross-section is denoted by $\delta(y)$.

The governing equations to be considered are the continuity, momentum and energy equations. Constant thermophysical properties are assumed, and natural convection is excluded. Then, the governing equations and the dimensionless variables will be similar to those documented in our previous paper [6] except for the hydraulic diameter which is now equal to the height of the duct for the polygonal cross-section. The solution domain is confined to the right half of the cross-section as shaded in Fig. 1(b). This is because of the condition of symmetry and also as a result of the utilization of the specific coordinate transformation methodology.

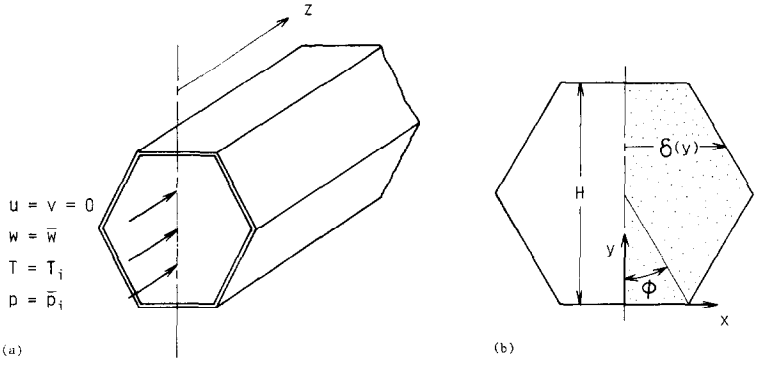

FIG. 1. (a) An axial coordinate of the regular polygonal duct. (b) A cross-section of the duct.

Numerical solutions

The solution methodology consists of two steps. The first step is to introduce a transformation of coordinates which maps the duct cross-section onto a rectangle. The second step is to reduce the three-dimensional problem, computationally, into a series of two-dimensional problems. The methodology for the first step is fully documented in earlier papers [6–8]. Specifically, the X, Y coordinates are transformed into η, ξ coordinates by the relation

$$\eta = X/\Delta(Y), \quad \xi = Y \text{ where } \Delta(Y) = \delta(y)/D_h. \tag{1}$$

The methodology to accomplish the second step is described by Patankar and Spalding [2]. A solution methodology for the *H1* boundary condition is described by Prakash and Liu [3].

Computations were performed with (16×30) grid points in the η–ξ plane. These grid points are distributed in a non-uniform manner with a higher concentration of grids close to the walls in both directions. Supplementary runs for $n = 6$ were performed with (10×18), (12×22), (16×30), (18×34), and (22×42) grid points to investigate grid size effects. The change in $(f\,Re)_{f.d.}$ between the coarse mesh (10×18) and the medium mesh (16×30) was 0.46% and between the medium mesh and the fine mesh (22×42) was 0.07%.

The first dimensionless step size $\Delta Z [= (\Delta z/D_h)/Re]$ is taken as 2×10^{-5}. Starting with this value, subsequent step sizes are gradually increased using the relation $\Delta Z = (1.1)$ (previous ΔZ) until $\Delta Z < (\Delta\eta)^2_{min}/10$, where $(\Delta\eta)_{min}$ is the minimum value of the control volume size in the η-direction. The maximum step size $\Delta Z = 1.1 \times 10^{-4}$, 7.6×10^{-5}, 3.9×10^{-5} and 2.4×10^{-4} for polygonal number $n = 4$, 6, 8 and ∞, respectively. This criterion was determined empirically to obtain a stable solution.

The axial step size is the controlling numerical parameter for the accuracy near the inlet. Therefore, supplementary runs were performed to investigate the step size effect for $n = 6$ and for the T boundary condition with the first step size as $\Delta Z = 2 \times 10^{-6}$ and the maximum step size as $\Delta Z = 7.6 \times 10^{-6}$. These step sizes were 1/10 of those used in the computations. The deviations of the average and the local Nusselt numbers (Nu_{mT} and Nu_T) at $(z/D_h)/(Re\,Pr) = 0.01$ for $Pr = 0.7$ are 1.5 and 0.3%, respectively. These deviations decrease with increasing axial length and Prandtl number.

RESULT AND DISCUSSIONS

Friction factor and pressure drop

The local friction factor f is defined as

$$f = \frac{(-d\bar{p}/dz)D_h/4}{(\rho\bar{w}^2)/2}. \tag{2}$$

In the fully developed region, the friction factor becomes inversely proportional to the Reynolds number, and $(f\,Re)$ becomes independent of z.

The computed values of the fully developed friction factors $(f\,Re)_{f.d.}$ are given in Table 1. Shih's [9] fully developed results are also listed. As seen from this table, the results of the present computation are in perfect agreement with those of Shih.

Table 1. Fully developed values of $(f\,Re)_{f.d.}$ and incremental pressure drop K

	$(f\,Re)_{f.d.}$		$K(\infty)$	
n	Present work	Shih [9]	Present work	Previous work
4	14.167	14.227	1.445	1.551 (Shah [10])
6	15.065	15.054	1.324	—
8	15.381	15.412	1.292	—
∞	15.925	16	1.253	1.25 (Prakash and Liu [3])

The pressure drop from the inlet up to z is defined as $\Delta p = p_i - \bar{p}(z)$ where p_i is the pressure at the inlet plane. This pressure drop can be expressed as

$$\frac{p_i - \bar{p}(z)}{(\rho\bar{w}^2)/2} = (f\,Re)_{f.d.}\left(\frac{4z}{D_h\,Re}\right) + K(z) \tag{3}$$

where $(f\,Re)_{f.d.}$ refers to the fully developed values, $(f\,Re)_{f.d.}(4z/D_h\,Re)$ represents the pressure drop if the flow were fully developed all the way from the inlet, and $K(z)$ is the incremental pressure drop due to the entrance effect. The asymptotic value of K for large z is called $K(\infty)$, and it represents the total incremental pressure drop due to the entrance effect. This value is obtained graphically by extrapolating the relationship between K and the axial distance and is summarized in Table 2. They are compared with the values obtained by Shah [10] for the square duct and Prakash and Liu [3] for the circular duct. The results indicate that the total incremental pressure drop $K(\infty)$ decreases with the polygonal number n.

Thermal results: isothermal duct—the T boundary condition

The T boundary condition corresponds to a uniform temperature T_w both axially and peripherally. The bulk temperature $T_b(z)$ at an axial location z is given by

$$T_b(z) = \frac{1}{\dot{m}C_p}\int_A C_p \rho w T\,dA \tag{4}$$

where C_p, $\dot{m}$, and A are the specific heat, total mass flow rate and the cross-sectional area, respectively. The heat transfer $Q(z)$ up to a distance z is equal to

$$Q(z) = \dot{m}C_p(T_b - T_i). \tag{5}$$

The average Nusselt number up to the axial location z and the local peripheral average Nusselt number at an axial location are defined as

$$Nu_{mT} = \frac{Q/(znH\tan\phi)D_h}{(\overline{T_w} - T_b)k}$$

$$Nu_T = \frac{(dQ/dz)D_h}{(T_w - T_b)k} \tag{6}$$

Table 2. Fully developed Nusselt number values for the developed and slug flows

	Nu_{mT}			Nu_{H1}		
	Developed flow		Slug flow	Developed flow		Slug flow
n	Present work	Previous work	Present work	Present work	Previous work	Present work
4	2.980	2.976 (Shah [10])	4.926	3.614	3.608 (Shah [10])	7.083
6	3.353	—	5.380	4.021	4.002 (Cheng [11])	7.533
8	3.467	—	5.526	4.207	4.153 (Cheng [11])	7.690
∞	3.654	3.657	5.769	4.367	4.364	7.962

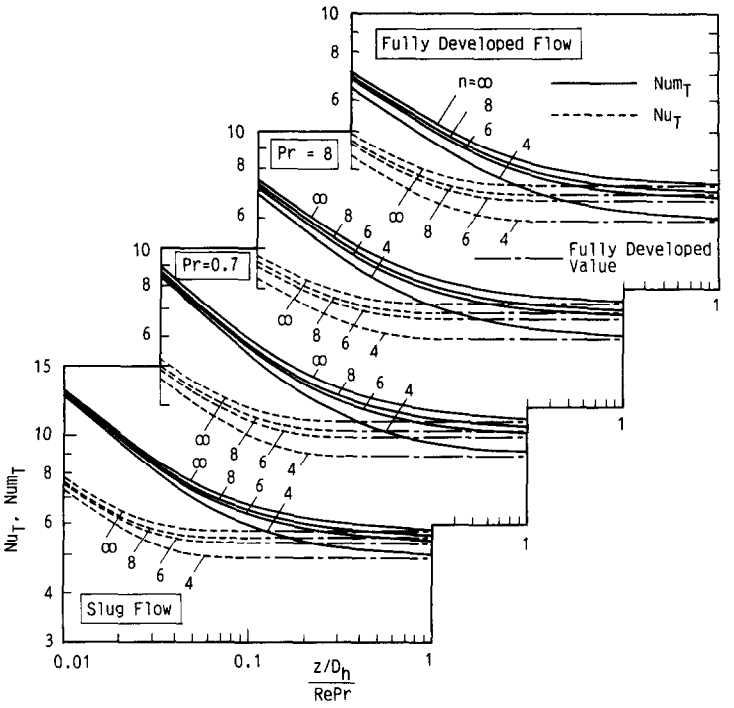

FIG. 2. Nusselt number with T boundary as a function of dimensionless axial length.

where k, ϕ and $(\overline{T_w - T_b})$ are thermal conductivity, duct angle and the log-mean temperature difference given by

$$\overline{T_w - T_b} = \frac{(T_w - T_i) - (T_w - T_b)}{\ln[(T_w - T_i)/(T_w - T_b)]}. \quad (7)$$

The fully developed Nusselt number values for the developed flow are listed in Table 2. Shah [10] did not present these values for the T boundary and for $n = 6$ and 8. The fully developed Nusselt number values for the slug flow are listed in Table 2. These values represent the results for very small Prandtl number ($Pr \ll 1$) and they differ from those obtained for the developed flow.

Results for the Nusselt number as a function of the dimensionless axial distance $[(z/D_h)/(Re\,Pr)]$ are plotted in Fig. 2 with the polygonal number n as a curve parameter. The dashed lines in the figure indicate the local peripheral average Nusselt number and the chain lines represent the fully developed values.

Thermal results: uniform heat input per unit axial length—H1 boundary

The local Nusselt number is defined as

$$Nu_{H1} = \frac{Q'/(nH\tan\phi)D_h}{(T_w - T_b)k} \quad (8)$$

where T_w is the wall temperature, which is uniform peripherally and T_b is the local bulk temperature given by equation (4).

The fully developed Nusselt number for the developed flow are listed in Table 2 as well as the values by Shih [9] and

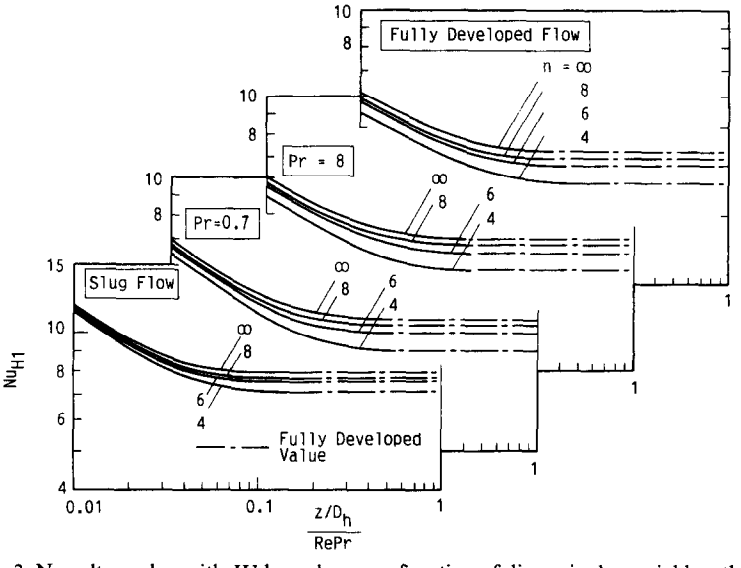

FIG. 3. Nusselt number with $H1$ boundary as a function of dimensionless axial length.

Cheng [11]. The present results are in good agreement with the values by Shah and Cheng. The fully developed Nusselt number values for the slug flow are also listed in Table 2. They differ from the values for the developed flow. Results for the Nu_{H1}, as a function of the dimensionless axial distance $[(z/D_h)/(Re\,Pr)]$, are plotted in Fig. 3 with the polygonal number n as a curve parameter. The fully developed Nusselt number values are also plotted in this figure by chain lines.

CONCLUDING REMARKS

Three-dimensional heat transfer and fluid flow characteristics in the entrance region of a polygonal duct are analyzed numerically by a coordinate transformation technique coupled with a calculation procedure for three-dimensional parabolic flows. The fully developed values of the Nusselt numbers and friction factors approach the available asymptotic results. The entry length results for the limiting case of a rectangular duct are in perfect agreement with the experimental and numerical results.

REFERENCES

1. R. K. Shah and A. L. London, *Laminar Flow Forced Convection in Ducts*. Academic Press, New York (1978).
2. S. V. Patankar and D. B. Spalding, A calculation procedure for heat, mass, and momentum transfer in three-dimensional parabolic flows, *Int. J. Heat Mass Transfer* **15**, 1787–1805 (1972).
3. C. Prakash and Ye-Di Liu, Analysis of laminar flow and heat transfer in the entrance region of an internally finned circular duct, *ASME J. Heat Transfer* **107**, 84–91 (1985).
4. K. C. Karki and S. V. Patankar, Heat transfer augmentation due to buoyancy effects in the entrance region of a shrouded fin array, *ASME J. Heat Transfer* **109**, 671–676 (1987).
5. A. Lawal and A. S. Mujumdar, Laminar flow and heat transfer in power-law fluids flowing in arbitrary cross-sectional ducts, *Numer. Heat Transfer* **8**, 217–244 (1985).
6. Y. Asako and M. Faghri, Three dimensional heat transfer and fluid flow characteristics in the entrance region of ducts of arbitrary cross-section, ASME paper 86-HT-12 (1986).
7. M. Faghri, E. M. Sparrow and A. T. Prata, Finite difference solutions of convection–diffusion problems in irregular domains using a non-orthogonal coordinate transformation, *Numer. Heat Transfer* **7**, 183–209 (1984).
8. M. Faghri and Y. Asako, Numerical determination of heat transfer and pressure drop characteristics for a converging–diverging flow channel, *ASME J. Heat Transfer* **109**, 606–612 (1987).
9. F. S. Shih, Laminar flow in axisymmetric conduits by a rational approach, *Can. J. Chem. Engng* **45**, 285–294 (1967).
10. R. K. Shah, Laminar flow friction and forced convection heat transfer in ducts of arbitrary geometry, *Int. J. Heat Mass Transfer* **18**, 849–862 (1975).
11. K. C. Cheng, Laminar flow and heat transfer characteristics in regular polygonal ducts, *Proc. Int. Heat Transfer Conf., 3rd AIChE*, New York, Vol. 1, pp. 64–76 (1966).

Int. J. Heat Mass Transfer. Vol. 31, No. 12, pp. 2593–2597, 1988
Printed in Great Britain

0017–9310/88 $3.00+0.00

Further results on evaporating bicomponent fuel sprays

SURESH K. AGGARWAL
Department of Mechanical Engineering, University of Illinois at Chicago, Chicago, IL 60680, U.S.A.

(*Received* 18 *November* 1987 *and in final form* 19 *May* 1988)

1. INTRODUCTION

IN A RECENT study [1], the vaporization behavior of a dilute multicomponent fuel spray in a hot laminar airflow was examined. Several liquid- and gas-phase models, which account for the diffusive–convective processes inside and outside the droplet, were investigated. It was indicated that while the effect of transient processes in the liquid is quantitative rather than qualitative for the single-component case, it can cause a more fundamental change in the gasification behavior of multicomponent fuel sprays. This is mainly due to the slow and often rate-controlling liquid mass diffusion process, and due to the volatility differential of the component fuels. It was further demonstrated that the effect of internal liquid motion is less important for the multicomponent case as compared to the single component, since the liquid motion can enhance the mass transport along the streamlines and not across them. The effects of several parameters were studied in the cited paper. However, the influence of three key parameters; namely the liquid Lewis number, volatility differential, and hot air stream temperature was not reported. In this paper, several additional results are presented, which focus on the influence of these parameters. In particular, the sensitivity of the spray vaporization behavior to the three liquid-phase models, namely the diffusion-limit, infinite-diffusion, and vortex models, is further examined as the above-mentioned parameters are varied.

The present study is important because the recommendation of the diffusion-limit model is based on two conditions. One is that the rate of liquid mass diffusion is extremely slow as compared to the droplet surface regression rate. The second is that there exists a substantial volatility differential in order for the liquid mass diffusion to be important. Thus, it is of interest to identify the range of dominant parameters such as the liquid Lewis number, environment temperature, and volatility differential, where the mass diffusion is indeed rate controlling.

2. THE DISCUSSION OF RESULTS

The physical model and the governing equations are described in an earlier paper [1]. Essentially, a transient one-dimensional bicomponent fuel spray in a hot airflow is considered. There are three subsets of equations; namely the gas-phase equations for the gas temperature, species mass fractions, velocity, and density; the liquid-phase equations for the position, velocity, and size of each group of droplets; and the droplet equations which govern the unsteady temperature and liquid mass fractions inside the droplet. These equations are solved by a hybrid Eulerian–Lagrangian explicit–implicit scheme.